EurJChem   European Journal of Chemistry

Check for updates

Antiproliferative potential, quantitative structure-activity relationship, cheminformatic and molecular docking analysis of quinoline and benzofuran derivatives

Praveen Kumar [iD] [1], Chinnappa Apattira Uthaiah [iD] [2], Santhosha Sangapurada Mahantheshappa [iD] [3], Nayak Devappa Satyanarayan [iD] [3], SubbaRao Venkata Madhunapantula [iD] [2], Hulikal Shivashankara Santhosh Kumar [iD] [4] and Rajeshwara Achur [iD] [1,*]

[1] *Department of Biochemistry, Kuvempu University, Jnana Sahyadri, Shimoga, Karnataka, 577451, India*
praveenbiochemku@gmail.com (P.K.), rajachur@gmail.com (R.A.)
[2] *Center of Excellence in Molecular Biology and Regenerative Medicine Laboratory, Department of Biochemistry, Jagadguru Sri Shivarathreeshwara Medical College, Jagadguru Sri Shivarathreeshwara Academy of Higher Education and Research, Mysuru, Karnataka, 570015, India*
auchinnappa16@gmail.com (C.A.U.), mvsstsubbarao@jssuni.edu.in (S.V.M.)
[3] *Department of Pharmaceutical Chemistry, Kuvempu University Post Graduate Centre, Kadur, Karnataka-577548, India*
santhosh.1507@rediffmail.com (S.S.M.), satya1782005@gmail.com (N.D.S.)
[4] *Department of Biotechnology, Kuvempu University, Jnana Sahyadri, Shimoga, Karnataka, 577451, India*
sk.genesan@gmail.com (H.S.S.K.)

* *Corresponding author at: Department of Biochemistry, Kuvempu University, Jnana Sahyadri, Shimoga, Karnataka, 577451, India.*
 e-mail: anr@kuvempu.ac.in *(R. Achur).*

RESEARCH ARTICLE

ABSTRACT

Quinoline and benzofuran moieties are commonly used for the synthesis of therapeutically beneficial molecules and drugs since they possess a wide range of pharmacological activities including potent anticancer activity as compared to other heterocyclic compounds. Many of well-known antimalarial, antimicrobial, anti-helminthic, analgesic, anti-inflammatory, antiprotozoal, and antitumor compounds contain quinoline/benzofuran skeleton. The aim of this study was to analyze ten new quinoline and eighteen benzofuran derivatives for carcinoma cell line growth inhibition and to predict possible interactions with the target. The anticancer activity of these compounds against colon cancer (HCT-116) and triple-negative breast cancer (MDA-MB-468) cell lines was determined and performed molecular docking to predict the possible interactions. Among ten quinoline derivatives, Q1, Q4, Q6, Q9, and Q10 were found to be the most potent against HCT-116 and MDA-MB-468 with IC_{50} values ranging from 6.2-99.6 and 2.7-23.6 μM, respectively. Using the IC_{50} values, a model equation with quantitative structure activity relationship (QSAR) was generated with their descriptors such as HBA1, HBA2, kappa (1, 2 and 3), Balaban index, Wiener index, number of rotatable bonds, log S, log P and total polar surface area (TPSA). The effect of benzofuran derivatives was moderate in cytotoxicity tests and hence only quinolines were considered for further analysis. The molecular docking indicated the mammalian / mechanistic target of rapamycin (mTOR), Topoisomerase I and II as possible targets for these molecules. The predicted results obtained from QSAR and molecular docking analysis of quinoline derivatives showed high correlation in comparison to the results of the cytotoxic assay. Overall, this study indicated that quinolines are more potent as anticancer agents compared to benzofurans. Further, compound Q9 has emerged as a lead molecule which could be the base for further development of more potent anticancer agents.

1. Introduction

Cancer remains a major health issue causing high rates of morbidity and mortality worldwide. In low and middle-income countries, approximately 70% of deaths occur due to cancer. GLOBOCAN 2018 estimates the global cancer burden to be 18.1 million deaths, among which lung cancer is the leading cause of death (18.4% of all cancer deaths) in men and women. Among women, breast cancer is the most frequently diagnosed cancer and the leading cause of cancer death [1].

Chemo- and radio-therapies are currently being used widely for treating cancer. These treatments are successful in a few cases, while in the majority of cases, it causes severe adverse effects that include drug-induced carcinoma, hepato-toxicity, tumorigenicity, and irritation of the skin due to lack of adequate target selectivity. Hence, novel anticancer drugs are being developed and selected by screening of combinatorial, chemical and virtual libraries, including small molecules, antibodies, peptides, and oligonucleotides [2].

Table 1. The cytotoxicity values of HCT-116 cells treated with quinoline and benzofuran derivatives for 24 hrs *.

Sample no	Code of compounds	Name	IC$_{50}$ (µM)
1	Q1	*N'*-((2-Chloroquinolin-3-yl) methylene)-2-(dimethylamino)acetohydrazide	8.5
2	Q2	*N'*-((2-Chloroquinolin-3-yl) methylene)-2-(diethylamino)acetohydrazide	ND
3	Q3	*N'*-((2-Chloroquinolin-3-yl) methylene)-2-(piperidin-1-yl)acetohydrazide	ND
4	Q4	*N'*-((2-Chloroquinolin-3-yl) methylene)-2-(4-methylpiperazin-1-yl)acetohydrazide	8.5
5	Q5	*N'*-((2-Chloroquinolin-3-yl) methylene)-2-morpholinoacetohydrazide	ND
6	Q6	*N'*-((6-Bromo-2-chloroquinolin-3-yl) methylene)-2- dimethylamino)acetohydrazide	6.474
7	Q7	*N'*-((6-Bromo-2-chloroquinolin-3-yl) methylene)-2-(diethylamino acetohydrazide	ND
8	Q8	*N'*-((6-Bromo-2-chloroquinolin-3-yl) methylene)-2-(piperidin-1-yl)acetohydrazide	ND
9	Q9	*N'*-((6-Bromo-2-chloroquinolin-3-yl) methylene)-2-(4-methylpiperazin-1-yl)acetohydrazide	99.6
10	Q10	*N'*-((6-Bromo-2-chloroquinolin-3-yl) methylene)-2-morpholinoacetohydrazide	6.254
11	B1	2-(Benzofuran-2-yl) quinoline-4-carboxylic acid	4.163
12	B2	2-(Benzofuran-2-yl)-6-chloroquinoline-4-carboxylic acid	23.56
13	B3	2-(Benzofuran-2-yl)-8-fluoroquinoline-4-carboxylic acid	9.34
14	B4	Methyl 2-(benzofuran-2-yl) quinoline-4-carboxylate	ND
15	B5	Methyl 2-(benzofuran-2-yl)-8-fluoroquinoline-4-carboxylate	5.099
16	B6	Methyl 2-(benzofuran-2-yl)-6-chloroquinoline-4-carboxylate	1.694
17	B7	Ethyl 2-(benzofuran-2-yl) quinoline-4-carboxylate	22.07
18	B8	Ethyl 2-(benzofuran-2-yl)-8-fluoroquinoline-4-carboxylate	22.86
19	B9	Ethyl 2-(benzofuran-2-yl)-6-chloroquinoline-4-carboxylate	1.392
20	B10	Butyl 2-(benzofuran-2-yl)-8-fluoroquinoline-4-carboxylate	2.770
21	B11	Butyl 2-(benzofuran-2-yl) quinoline-4-carboxylate	ND
22	B12	Butyl 2-(benzofuran-2-yl)-6-chloroquinoline-4-carboxylate	ND
23	B13	Propyl 2-(benzofuran-2-yl) quinoline-4-carboxylate	ND
24	B14	Propyl 2-(benzofuran-2-yl)-8-fluoroquinoline-4-carboxylate	ND
25	B15	Propyl 2-(benzofuran-2-yl)-6-chloroquinoline-4-carboxylate	ND
26	B16	Isopropyl 2-(benzofuran-2-yl) quinoline-4-carboxylate	ND
27	B17	Isopropyl 2-(benzofuran-2-yl)-8-fluoroquinoline-4-carboxylate	ND
28	B18	Isopropyl 2-(benzofuran-2-yl)-6-chloroquinoline-4-carboxylate	ND
29	*Cis*-platin	*Cis*-platin	9.1

* Serial numbers 1 to 10 are quinoline derivatives and 11 to 28 are benzofuran derivatives. Serial number 29 is *cis*-platin, positive control drug. ND: Not determined.

Most anticancer drugs such as mammalian/mechanistic target of rapamycin (mTORC1) inhibitors induce autophagy; however, it remains unclear whether autophagy increases their antitumor properties or leads to therapeutic resistance [3]. Radiation therapy is another treatment option for cancer. The patient is treated by the use of high intense radiation doses to kill cancer cells to reduce tumours. Radiation treatment kills or slows growth of cancer cells by damaging DNA. However, studies have shown that radiation therapy does not immediately kill cancer cells [4]. In the beginning of 20th century, the use of chemotherapy to treat cancers began with attempts to narrow the adverse effect of chemicals that could selectively affect the disease by developing methods for screening chemicals using rodent tumour models [5]. However, cancer treatment using nonspecific chemotherapeutic agents is likely to cause severe adverse effects.

Several analogues of quinoline have been reported experimentally and clinically over the past decade, exhibiting various biological activities [6]. Chloroquine and hydroxy-chloroquine are the class of antimalarial drugs that suppress autophagy, resulting in increased cytotoxicity in preclinical models when used in conjunction with several anticancer drugs. Benzofuran derivatives display a wide range of biological activities including, analgesic, anti-inflammatory [7], cardiovascular function and anticancer activities [8]. Thus, quinolines and benzofurans are representatives of a large variety of anticancer agents [9]. Recent studies have shown that quinoline and its analogues can inhibit tyrosine kinases, proteasome and mTOR [10]. Keeping this in view, in this study, we analysed a series of novel quinoline and benzofuran analogues in relation to their biological activities, action mechanisms, structure-activity relationship (SAR), as well as selective and precise activity against various cancer targets.

2. Experimental

2.1. Synthesis of quinoline and benzofuran derivatives

Among the two classes of compounds, the quinoline derivatives (Q1 to Q10) were recently synthesized in our labo-

ratory. Briefly, the 2-amino-*N'*-((2-chloroquinolin-3-*yl*)methyl ene)acetohydrazide derivatives were synthesized by reacting chloroquinoline-3-carbaldehyde with hydrazine hydrate to yield the corresponding hydrazide which upon reacting with chloroacetyl chloride, yields 2-chloro-*N'*-((2-chloroquinolin-3-*yl*)methylene)acetohydrazide which upon further treatment with secondary amines produces the target compounds [11] (unpublished data, manuscript communicated) (Table 1 and Figure 1). The benzofuran derivatives (B1 to B18) were synthesized by using 2-acetyl benzofuran and different substituted isatin as per the published procedure [12]. The carboxylic acid functionality of 2-(1-benzofuran-2-yl) quino line-4-carboxylic acid was further used in the synthesis of different esters of aliphatic alcohols in acidic medium (Table 1).

2.2. Cytotoxicity assessment of quinoline and benzofuran derivatives

All the selected compounds were dissolved in 1% dimethyl sulfoxide (DMSO) and diluted with media to the desired concentrations. Colorectal and breast cancer cell lines (HCT-116 and MDA-MB-468) were procured from National Center for Cell Science (NCCS, Pune, Maharashtra, India) and were grown in high glucose DMEM supplemented with 10% fetal bovine serum. The cell viability was determined by using Sulforhodamine B (Sigma Chemical Company, St. Louis, USA) assay. The optical density was determined using multimode plate reader (EnSpire, Perkin Elmer, Inc.) at a wavelength of 515 nm. Cell culture reagents and disposables were procured from Life Technologies, Carlsbad, CA, USA, and Tarsons India Pvt Ltd, Mumbai, Maharashtra, India. AutoDockTools 1.5.6 software [13] was from The Scripps Research Institute, North Torrey Pines Road, La Jolla, CA.

The protein-binding dye Sulforhodamine B (SRB) assay has been used to perform various screening assays inexpensively to investigate cytotoxicity in cell-based studies to measure the cell growth as described earlier [14]. The protocol has been optimized for the *in vitro* screening of synthesized quinoline and benzofuran analogues with adherent cancer cells in 96-well format [15].
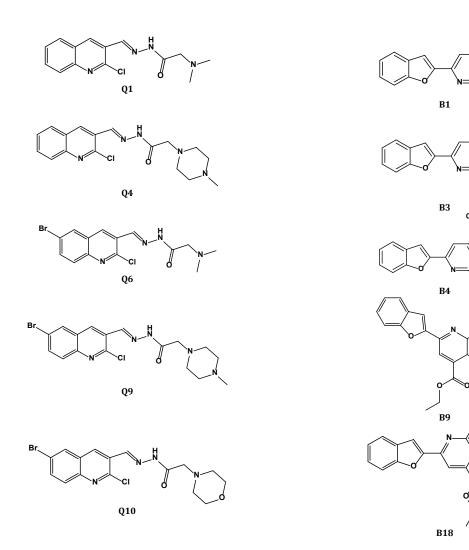
Figure 1. Structure of eight hit derivatives of quinoline and benzofuran as identified by cytotoxicity assay. Q1, Q4, Q6, Q9 and Q10 are quinoline derivatives. B1, B3, B4, B9 and B18 are benzofuran derivatives.

In this study, a series of 10 quinoline and 18 benzofuran analogues were screened against human cancer cell lines HCT-116 (Colorectal carcinoma) and MDA-MB-468 (Triple negative breast cancer, TNBC) *in vitro*. The cell lines were grown in high glucose DMEM supplemented with 10% fetal bovine serum, 2 mM L-glutamine, 10,000 units/mL penicillin G sodium, 10 mg/mL streptomycin sulphate in a humidified 5% CO$_2$ atmosphere and incubated at 37 °C. The HCT-116 cells were initially exposed to these quinoline and benzofuran derivatives to identify the potential lead molecules. Based on this, selected eight derivatives were used for treating with breast cancer cell line MDA-MB-468 and colorectal carcinoma HCT-116 cells, in a dose and time dependent manner. After the incubation period, the cells were fixed using 50% cold aqueous trichloroacetic acid (TCA). The plates were incubated for 1 h at room temperature, washed with tap water, and air-dried. To the dried plates, 100 μL 0.4% SRB solution was added to stain the cells. Through washing with 1% aqueous acetic acid, free SRB was extracted. The plates were air-dried, and the attached dye was dissolved by adding 100 μL of 10 mM Tris base buffer (pH = 7.2). The plates were placed on a shaker for 5 min prior to analysis. The optical density was determined by using multimode plate reader (EnSpire, Perkin Elmer Inc.) at a wavelength of 515 nm. Cell viability percentage was calculated using the following equation.

$$\% \text{ Viability} = 100 - \left[\left\{ \frac{(OD \text{ of Control} - OD \text{ of Sample})}{(OD \text{ of Control})} \right\} \times 100 \right] \quad (1)$$

Further, the IC$_{50}$ value, which is the concentration of a drug necessary for 50% inhibition was determined. From the % viability data, the IC$_{50}$ value was calculated for the HCT-116 and MDA-MB-468 cell line which is a measure of compound efficacy. Non-linear regression analysis of log (inhibitor) versus standardized dose-response plots were used to determine the IC$_{50}$ values. The values are the mean (SEM) of triplicate experiments.

2.3. Quantitative structure-activity relationship model development and validation

In the present study, quantitative structure-activity relationship (QSAR) modeling was performed based on the cytotoxicity data generated using benzofuran and quinoline analogues against colorectal carcinoma cell line, HCT-116. The BuildQSAR [16] version 2.1.0 was used to generate QSAR model equation. The structure of these ten quinoline and eighteen benzofuran analogues was drawn using Chem3D 15.0 software. The chemical, structural, and pharmacophore descriptors were calculated by using Chemdes web server [17] and Chem3D 15.0 [18].
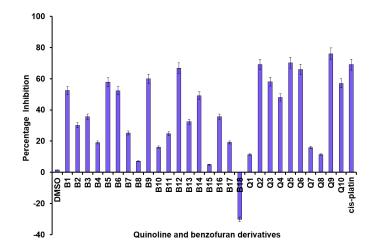
Figure 2. Effect of selected quinoline and benzofuran derivatives against colorectal carcinoma HCT-116 cells viability. HCT-116 cells were exposed to benzofuran (B1 to B18) and quinoline (Q1 to Q10) derivatives at 100 μM concentration for 24 h and the cell viability assessed by SRB assay.

To choose the constructive descriptors with the biological activity of these molecules, highly correlated descriptors were selected to build a best QSAR model with multiple linear regression method.

2.4. Ligand preparation and analysis

The benzofuran and quinoline molecular structures were drawn with Marvin Sketch and the SMILES format was extracted for all the molecules. The SMILES format was submitted for target prediction at Swiss Target Prediction server (http://www.swisstargetprediction.ch/) [19]. The SMILES were also submitted for Molinspiration server (https://www.molinspiration.com/cgi-bin/properties) [20] for predicting the bioactivity and drug likeness. All ligands were subjected to energy minimization and PDBQT file was generated using PRODRG (http://prodrg1.dyndns.org/submit.html) web server [21].

2.5. Molecular docking and analysis

For molecular docking, the structure of target receptor proteins was obtained from the Protein Data Bank [22] (PDB code: 4JSV, 1T8I and 1ZXM) and visualized with Chimera 5.3.1 software (RBVI, Resource for Biocomputing, Visualization, and Informatics, University of California, CA, USA, www.cgl.ucsf.edu/chimera/) [23]. The structure of compounds was prepared with MarvinSketch 5.5 software (Marvin, version 5.5.0.1, Program B, ChemAxon, Budapest, Hungary; www.chemaxon.com/products) which was energy minimized and protonated (pH = 7.4) with OpenBabel 2.2.3 software (Version 2.2.3, http://openbabel.org), using the MMFF94s force field [24]. Docking studies were performed with AutoDock 4.2 software (http://autodock.scripps.edu/) provided with AutoDock Tools 1.5.4 graphical interface. The grid box was centered for 4JSV receptor at x = 11.11, y = 18.23 and z = 15.33. Docking pose was obtained through Lamarckian genetic algorithm search engine. For the analysis of receptor-ligand interactions, a virtual screening pipeline was designed. The ligands were prepared using PRODRG server and the receptor file was taken from PDB database. The PyRx was used for the virtual screening pipeline. PyRx was installed with Python 7.2 and Auto Dock Vina was integrated by specifying the executable file path of Auto Dock Vina into PyRxsuite [25]. The post-docking analysis was done with BIOVIA DS [26] view which helps to generate the docking poses in 2D image format along with proper interaction specifications.

2.6. Cheminformatics based cluster analysis of quinoline and benzofuran ligands

A molecular descriptors-based clustering analysis was performed with the properties of ligands, which includes molecular weight, lipophilicity (cLogP), the aqueous solubility (cLogS), Hydrogen bond acceptors/donors, polar surface area, and drug likeness. In order to assess the toxicity prediction's reliability, such as mutagenic, tumorigenic, reproductive effective and irritant nature of the compounds, the PAST (Paleontological Statistics Software) package for education and data analysis tool was used for the cheminformatics-based cluster analysis [27,28].

3. Results

3.1. Cytotoxic effect of quinoline and benzofuran analogues on colorectal and breast cancer cell lines

Initially, all the novel quinoline and benzofuran analogues used in this study were evaluated for their cytotoxicity against HCT-116 colorectal carcinoma to identify the potent lead molecules by using SRB (Sulforhodamine B) assay. According to the cytotoxicity data, ten quinoline and eighteen benzofuran derivatives displayed variable efficacy in inhibiting the growth of human tumour cell lines HCT-116 (Table 1, Figure 2). Based on this data, selected potent three benzofuran and five quinoline molecules were tested for their efficacy using triple negative breast cancer cell line, MDA-MB-468 in the concentration range 10 μM to 1000 mM (Figure 3). Among the tested quinolines, compound Q9, (*N'*-[(6-bromo-2-chloro quinolin-3-yl)methylidene]-2-(4-methylpiperazin-1-yl) aceto hydrazide) with 6-bromo substituent in the benzo ring of 2-chloroquinolin-3-yl moiety, was found to be the most potent. Compound Q9 exhibited a broad-spectrum cytotoxic efficacy in colon and breast cancer cells, with IC$_{50}$ values ranging from 29.8 to 99.9 μM. Further, based on this, the compound Q9 was subjected to efficacy test in both colorectal carcinoma HCT-116 and MDA-MB-468 cells in a dose and time dependant manner in the concentration range 3.9 to 500 μM at 24, 48 and 72 hrs exposure time (Figure 4).

3.2. QSAR analysis

In order to find the best descriptors to construct a model, it is important to eliminate unnecessary descriptors to generate a significant model [29].
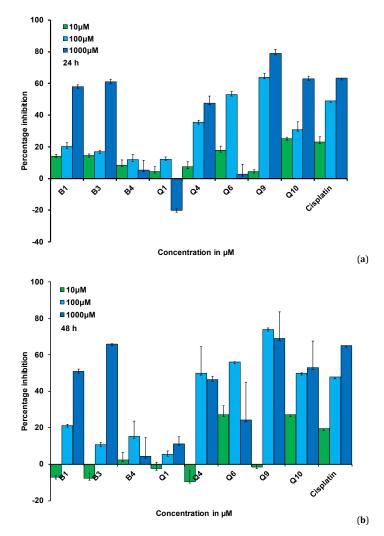
Figure 3. Effect of selected five quinoline and three benzofuran derivatives on the growth of breast cancer cell line MDA-MB-468. (**a**), Treated for 24 hours (**b**), for 48 hours. All values are expressed in triplicate averages ± SD. *Cis*-platin was used as the positive control.

In the present study, although we subjected all the 28 molecules for cytotoxic assessment and QSAR analysis, 8 molecules did not show parameters to generate significant QSAR equation and these outliers have been deleted. Thus, QSAR modelling was performed using a total of 20 compounds with recorded anticancer activity against the human colorectal cancer cell line, HCT-116. For each compound, a total of thirteen chemical descriptors (Physico-chemical properties) were determined [30]. The selection was made based on similarities between the structural / pharmacophore or chemical groups. Similarly, highly correlated descriptors were chosen to select the best subset of descriptors. Ultimately, a model was developed based on the multiple linear regression method.

3.3. QSAR model equation

The multiple linear regression based QSAR model for the inhibitory activity of a series of six quinoline and fourteen benzofuran derivatives against colorectal carcinoma (HCT-116) cells was validated. The QSAR model equation is given below.

$\text{Log } 1/ \text{ IC}_{50} (\mu M) = -0.9671 (\pm 0.4081) \text{ HBA } 1 - 0.6793$
$(\pm 0.9124) \text{ KAPPA1} + 4.7242 (\pm 2.0044) \text{ KAPPA2} - 0.0059$
$(\pm 0.1004) \text{ TPSA} + 13.7902 (\pm 16.1787)$

$(n = 20; R = 0.901; s = 1.337; F = 16.267; p < 0.0001; Q2 = 0.565;$
$\text{SPress} = 2.036; \text{SDEP} = 1.809)$ (2)

The derived QSAR equation showed a significant relationship between IC$_{50}$ and descriptors. The standard deviation of predictions, SPRESS, is calculated from PRESS, the sum of the squared errors of these predictions, considering the number of degrees of freedom. SDEP (the standard deviation of the error of predictions) corresponds to SPRESS but the number of degrees of freedom is not considered in the calculation of the SDEP value. The smallest SPRESS or SDEP value has been taken as the criterion for the optimum number of components. The Q2 value suggests the ability of model to give a precise forecast. SPRESS values suggest the statistical importance of the model for predicting behavior. The regression coefficient value ($r^2 = 0.8127$) indicates the correlation between the inhibitory activity and the chemical descriptors in the data set (Figure 5). The coefficient analysis of QSAR model reveals that the descriptors HBA 1 and KAPPA2 are statistically significant with the cytotoxic activity of the molecules. The obtained QSAR model provided a consistent relationship between the properties of the chemical structure as descriptors and the compound inhibitory activities. In essence, QSAR uses different structural descriptors to link them to the particular action of compounds.
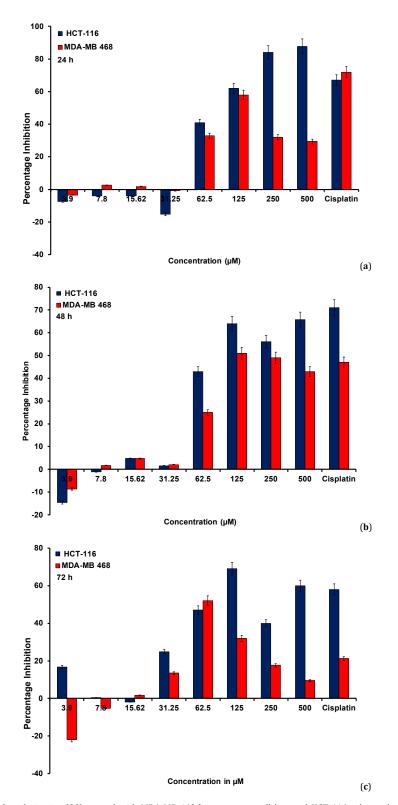
Figure 4. Effect of hit quinoline derivative (Q9) treated with MDA-MB-468 breast cancer cell line and HCT-116 colorectal cells in both time and dose dependent manner (**a**), Treated for 24 hours (**b**), Treated for 48 hours, (**c**) Treated for 72 hours. All values are expressed in triplicate averages ± SD. *Cis*-platin was used as the positive control.

3.4. Cheminformatics based cluster analysis of quinoline and benzofuran ligands

The descriptor-based clustering of quinolines yielded two major clusters, where Q7-Q10 formed one cluster and Q1-Q6 made another one (Table 2 and Figure 6). All quinoline ligands were found to have clogP values of less than 4, which indicate that they are potent drug candidates within the recommended range. The latter cluster formed two sub-clusters, one comprising Q3-Q6 and the other comprising Q1 and Q2. The ligands Q2 and Q7 were found to have an irritation effect.

Table 2. Cheminformatics analysis of a series of 10 quinoline analogues.

Comp.	Molecular weight (dal)	cLogP [a]	cLogS [b]	Hydrogen Acceptors	Hydrogen Donors	Polar surface area [c]	Drug-likeness [d]	Mutagenic	Tumorigenic	Reproductive effective	Irritant
Q1	290.753	2.0707	-2.88	5	1	57.59	6.2876	0	0	0	0
Q2	318.807	2.8833	-3.48	5	1	57.59	8.4531	0	0	0	High
Q3	345.833	2.1491	-2.45	6	1	60.83	11.304	0	0	0	0
Q4	345.833	2.1491	-2.45	6	1	60.83	11.304	0	0	0	0
Q5	369.649	2.7959	-3.71	5	1	57.59	4.4976	0	0	0	0
Q6	369.649	2.7959	-3.71	5	1	57.59	4.4976	0	0	0	0
Q7	409.714	3.9289	-4.67	5	1	57.59	3.17	0	0	0	1
Q8	409.714	3.9289	-4.67	5	1	57.59	3.17	0	0	0	0
Q9	411.686	2.7649	-3.78	6	1	66.82	3.6664	0	0	0	0
Q10	411.686	2.7649	-3.78	6	1	66.82	3.6664	0	0	0	0

[a] cLogP: The logarithm of partition coefficient between *n*-octanol and water (log of octanol/water).
[b] cLogS: The logarithm of solubility, HBA and HBD (Number of H atom donors and acceptors).
[c] TPSA: Total polar surface area.
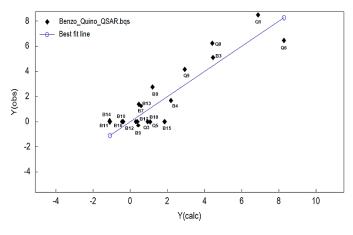[d] Drug-likeness: Drug-likeness properties of a molecule.

Figure 5. Plot of observed and calculated cytotoxic effect of quinoline and benzofuran analogues as determined by the QSAR model. Abbreviation: calc: Calculated; and obs: Observed.
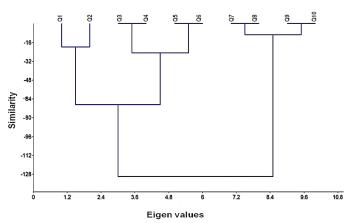

Figure 6. Cheminformatics based cluster analysis of quinoline ligands.

This shows that, although the compounds belong to the same class, the difference in their properties with respect to drug likeness parameters does exist. This is evident in the pharmacodynamic simulation results of the ligand's interaction with its mTOR protein and topo I and II target receptors. This could be one of the main reasons for the differential response of the ligands in terms of their binding efficiency to the receptor. However, among all the ligands, Q9 was found to exhibit the most favourable SAR values and the docking analysis also confirmed this with better binding statistics.

Similarly, the cluster analysis of benzofuran ligands based on the pharmacophore descriptors was carried out. The ligands were grouped into two broad clusters comprising 8 ligands in one cluster and 10 ligands in another cluster. The analysis yielded two major clusters in which B12-B17 (total eight ligands) having high similarity formed one cluster and B4-B15

(total ten ligands) having multiple branches formed another (Table 3 and Figure 7). Out of 18 molecules B9, B10, B11 and B12 ligands were predicted to show irritation effect. Ligands B11, B10, B9, B12 and B18 were found to have clogP values more than 5, which violate the rule of five for drug likeness. Hence, the feasibility of these benzofurans to serve as good drug candidates is unlikely. However, all the ligands were subjected to docking analysis.

3.5. Molecular docking studies of quinoline and benzofuran analogues

The molecular docking studies were performed to investigate the binding mode into the active site of three different receptor proteins reported to be expressed at elevated levels in cancer cells.

Table 3. Cheminformatics analysis of a series of 18 benzofuran analogues.

Comp.	Molecular Weight (dal)	cLogP [a]	cLogS [b]	Hydrogen Acceptors	Hydrogen Donors	Polar surfaces area [c]	Drug-likeness [d]	Mutagenic	Tumorigenic	Reproductive effective	Irritant
B1	325.75	3.87	-4.6	4	1	59.42	-0.27	0	0	0	0
B2	325.75	3.9	-4.6	4	1	59.42	-0.27	0	0	0	0
B3	305.33	3.7	-3.9	4	0	48.42	-2.63	0	0	0	0
B4	305.33	3.68	-3.9	4	0	48.42	-2.63	0	0	0	0
B5	339.78	4.3	-4.7	4	0	48.42	-2.52	0	0	0	0
B6	339.78	4.3	-4.7	4	0	48.42	-2.52	0	0	0	0
B7	337.34	4.2	-4.6	4	0	48.42	-5.65	0	0	0	0
B8	337.35	4.2	-4.6	4	0	48.42	-5.65	0	0	0	0
B9	365.40	5.1	-5.1	4	0	48.42	-6.68	0	0	0	3
B10	365.40	5.1	-5.1	4	0	48.42	-6.68	0	0	0	3
B11	381.89	5.6	-5.5	4	0	48.42	-5.22	0	0	0	3
B12	381.86	5.6	-5.5	4	0	48.42	-5.22	0	0	0	3
B13	351.38	4.6	-4.8	4	0	48.42	-1.94	0	0	0	0
B14	351.38	4.6	-4.8	4	0	48.42	-1.94	0	0	0	0
B15	333.39	4.5	-4.6	4	0	48.42	-3.06	0	0	0	0
B16	333.39	4.5	-4.6	4	0	48.42	-3.06	0	0	0	0
B17	367.83	5.0	-5.4	4	0	48.42	-2.94	0	0	0	0
B18	367.83	5.1	-5.4	4	0	48.42	-2.94	0	0	0	0

[a] cLogP: The logarithm of partition coefficient between *n*-octanol and water (log of octanol/water).
[b] cLogS: The logarithm of solubility, HBA and HBD (Number of H atom donors and acceptors).
[c] TPSA: Total polar surface area.
[d] Drug-likeness: Drug-likeness properties of a molecule.

Table 4. Binding affinity and interactions of quinoline ligands with mTOR receptor (PDB: 4JSV).

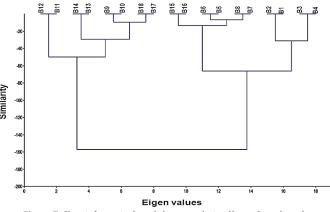| Compound	Binding energy	Ligand efficiency	Inhibition constant (μM)	No of H-bonds	Amino acids in the binding site	H-bond length (Å)
Q_1	-6.69	-0.33	12.40	1	LYS-2187	1.812
Q_2	-5.65	-0.26	66.98	2	LYS-2197	1.938
					SER-2342	1.896
Q_3	-6.51	-0.28	16.90	2	LYS-2197	2.140
					SER-2342	2.020
Q_4	-6.77	-0.28	10.86	-	-	-
Q_5	-5.79	-0.25	57.45	-	-	-
Q_6	-6.17	-0.29	28.60	1	SER-2342	1.923
Q_7	-5.72	-0.25	63.92	1	LYS-2187	1.904
Q_8	-3.41	-0.14	-3190	-	-	-
Q_9	-7.18	-0.29	5.47	2	LYS-2187	1.903
					ASP-2357	2.066
Q_{10}	-6.70	-0.28	12.36	-	-	-

Figure 7. Cheminformatics based cluster analysis of benzofuran ligands.

They are a mammalian target of rapamycin (also known as mechanistic target of rapamycin or mTOR), topoisomerase I, and topoisomerase II, having PDB Codes 4JSV, [31] 1T8I [32] and 1ZXM [33], respectively.

Initially, a series of a ten quinoline and eighteen benzofuran derivatives were docked with mTOR receptor, followed by comparison of predicted binding affinities with the receptor mTOR (PDB 4JSV). Based on each protein's experimental resolution data, the three-dimensional (3D) structures of compounds or ligands were generated according to Gaussian theory [34] for a geometrical optimization method. All the structured conformations on the potential energy surface have been verified as minimal. The docking simulations for the collection of optimized ligands were conducted using the software AutoDock v.4.2. [35]. The quinoline ligands, Q1, Q2, Q3, Q6, Q7 and Q9 were found to have good interaction with target receptor to form hydrogen bonds. The cluster and docking analysis suggest that, the ligand Q8 has poor binding statistics as compared to Q9, which bears best binding statistics among all the quinoline ligands. The other compounds, Q4, Q1 and Q10 also showed binding statistics close to that of Q9. The compound Q9 predicted to have significant binding affinity toward smTOR with a docking score of -7.18 kcal/mol, which has revealed the formation of two hydrogen bonds with the binding pocket residues, ASP-2357 (1.903 Å) and LYS-2187 (2.066 Å). The other molecules, whereas Q1 and Q7 both found to interact with LYS-2187, with a binding energy ranging from -6.7 to -3.41 kcal/mol (Table 4 and Figure 8).

Table 5. Binding affinity and interactions of benzofuran ligands with mTOR receptor (PDB: 4JSV).

Compound	Binding energy	Ligand efficiency	Inhibition constant (μM)	No of H-bonds	Amino acids in the binding site	H-bond length (Å)
B3	-7.20	-0.32	6.56	2	LYS2187	1.794
					ASP2357	1.950
B1	-7.07	-0.26	40.26	2	LYS2187	1.895
					ASP2357	2.202
B5	-7.00	-0.31	5.28	0	-	-
B4	-6.83	-0.30	9.81	1	ASP2357	2.078
B9	-6.75	-0.29	9.16	1	LYS2187	1.794
B12	-6.60	-0.23	93.04	0	-	-
B17	-6.51	-0.25	38.78	1	LYS2187	2.062
B16	-6.78	-0.24	48.68	0	-	-
B14	-6.70	-0.27	11.30	0	-	-
B18	-6.07	-0.20	93.84	1	LYS2187	1.962
B7	-6.02	-0.21	94.38	1	SER2165	
B2	-6.60	-0.25	14.49	1	ASP2357	1.842
B8	-6.78	-0.23	49.84	0	-	-
B13	-6.35	-0.29	33.29	0	-	-
B15	-5.78	-0.22	63.20	0	-	-
B6	-5.79	-0.26	19.10	0	-	-
B10	-6.29	-0.25	16.91	0	-	-
B11	-6.06	-0.23	35.81	0	-	-

Table 6. Binding affinity and interactions of quinoline ligands against human DNA Topoisomerase I (PDB-1T8I).

Compound	Binding energy	Ligand efficiency	Inhibition constant (μM)	No of H-bonds	Amino acids in the binding site	H-bond length (Å)
Q_1	-4.20	-0.22	678.19	3	ARG-364	1.968
					ARG-364	2.229
					ASP-533	1.920
Q_2	-3.34	-0.15	3555	1	ASP-533	2.190
Q_3	-4.06	-0.18	1050	2	ARG-364	1.931
					ASP-533	1.987
Q_4	-4.21	-0.18	8.18	1	ASP-533	1.740
Q_5	-4.21	-0.18	814.61	3	ARG-364	2.131
					LYS-532	2.199
					ARG-364	2.171
Q_6	-3.57	-0.17	2410.00	1	PTR-723	2.120
Q_7	-4.37	-0.19	622.48	1	ARG-364	1.880
Q_8	-5.23	-0.22	145.98	1	ASP-533	1.820
Q_9	-3.98	-0.16	1200.00	2	THR-718	1.675
					THR-718	1.902
Q_{10}	-5.00	-0.21	216.42	4	LYS-532	2.200
					LYS-532	1.910
					ARG-364	2.139
					ASP-533	2.160

Table 7. Binding affinity and interactions of quinoline ligands against human DNA Topoisomerase II (PDB-1ZXM).

Compound	Binding energy	Ligand efficiency	Inhibition constant (μM)	No of H-bonds	Amino acids in the binding site	H-bond length (Å)
Q1	-5.38	-0.27	114.76	1	GLN655	2.220
Q2	-7.94	-0.36	1.51	-	-	-
Q3	-4.06	-0.18	1050.00	-	-	-
Q4	-9.49	-0.40	0.198	-	-	-
Q5	-7.15	-0.31	5.79	2	TRP407	2.023
					SER657	1.949
Q6	-6.83	-0.30	9.88	1	SER657	2.046
Q7	-6.36	-0.28	21.62	2	GLN655	2.215
					PHE653	2.150
Q8	-7.02	-0.29	7.16	2	PHE653	1.704
					GLN655	1.906
Q9	-6.78	-0.27	10.72	3	GLU719	2.147
					SER665	1.921
					LYS666	1.913
Q10	-6.95	-0.29	8.11	3	TRP407	2.111
					GLN655	2.208
					GLN665	2.187

Among benzofurans, the ligand B18 formed one H-bond with the residue LYS-2187 (1.962 Å), whereas B1 and B3 formed two hydrogen bonds with LYS-2187 and ASP-2357. Although the benzofuran analogues B1, B3, B4, B9 and B18 showed good binding affinities ranging from -7.7 to -5.78 kcal/mol with significant docking score and hydrogen bond formation, the screening of these with mTOR showed moderate binding statistics as compared to quinolines (Table 5 and Figure 9). Keeping in view of this ability of quinolines as compared to benzofurans, only the quinolines were selected for further docking analysis with topoisomerase I and II. The analysis of docking results and binding pattern of all the ten quinolines (Q1-Q10) were found to interact with the important residues, ARG-364, ASP-533 and THR-718 of topo I DNA complex protein (PDB 1T8I). The docking score and interaction parameters of these are given in Table 6. The ligands Q1, Q5, Q9 and Q10 formed two to four hydrogen bonds with a binding energy of -4.20, -4.21, -3.98 and -5.0 Kcal/mol, respectively (Figure 9). Similarly, the binding interaction and docking results of all quinoline molecules with topo II DNA complex protein (PDB 1ZXM) revealed that Q7, Q8, Q9 and Q10 ligands established two to three hydrogen bonds with topoisomerase II receptor 1ZXM.
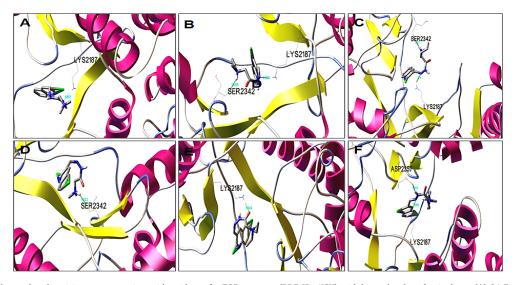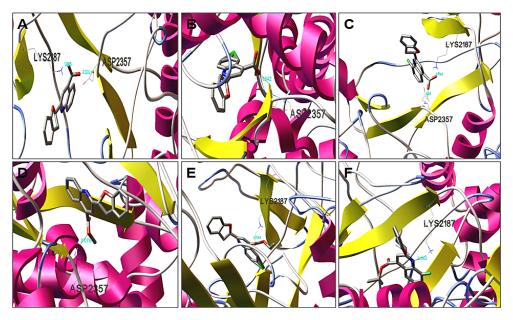
Figure 8. Hydrogen bond positions among amino acid residues of mTOR receptor (PDB ID: 4JSV) with hit molecules of quinolines. (A) Q1 Formed H-bond with LYS-2187 (1.812 Å) (B) Q2 Formed H-bond with LYS-2187 and SER-2342 (1.938 and 1.896 Å) (C) Q3 Formed H-bond with LYS-2187 and SER-2342 (2.14 and 2.02 Å) (D) Q6 Formed H-bond with SER-2342 (1.923 Å) (E) Q7 Formed H-bond with LYS-2187 (1.904 Å) (F) Q9 Formed H-bond with ASP-2357 and LYS-2187 (1.903 and 2.066 Å). Abbreviation: PDB, Protein Data Bank, mTOR-mammalian/ mechanistic target of Rapamycin.

Figure 9. Hydrogen bond positions among amino acid residues of mTOR receptor (PDB ID: 4JSV) with hit molecules of benzofuran. (A) B3 Formed H-bond with LYS-2187 and ASP 2357 (1.794 and 1.95 Å), (B) B1 Formed H-bond with LYS-2187 and ASP 2357 (1.897 and 2.2 Å), (C) B4 Formed H-bond with ASP-2357 (2.078 Å), (D) B9 Formed H-bond with LYS-2187 (1.794 Å), (E) B17 Formed H-bond with LYS-2187 (2.062 Å), (F) B18 Formed H-bond with LYS-2187 (1.962 Å). Abbreviation: PDB, Protein Data Bank, mTOR-Mammalian Target of Rapamycin.

Among these, the molecule Q9 was found to have best binding energy (-6.78 Kcal/mol) and able to form three hydrogen bonds with GLU-719, SER-665 and LYS-666 residues (Table 7).

4. Discussion

In this study, we have analyzed the cytotoxic ability of a series of quinoline and benzofuran derivatives using *in silico* and *in vitro* approaches which demonstrated the possibilities of development of promising novel anticancer agents. Several compounds bearing quinoline moiety, such as Bosutinib and Anlotinib, are already being used in clinical practice to fight against cancer [36]. Similarly, a novel series of benzofuran derivatives has shown higher inhibitory effects against MDA-MB-468 human breast cancer cells [37]. The quinoline moiety has become one of the most privileged structural motifs in the

discovery of anticancer agent and the present study findings are in concordance with previous studies [36]. Among all the tested quinoline and benzofuran analogues, the data obtained in this study has revealed that a quinoline derivative Q9, with the nomenclature *N'*-(6-bromo-2-chloroquinolin-3-yl)methyldene-2-(4-methylpiperazin-1-yl)acetohydrazide) possess highly significant cytotoxicity against colorectal carcinoma (HCT-116) and triple negative breast cancer cell line (MDA-MB-468) with an IC_{50} values ranging from 4.1 to 99.6 μM.

The quantitative structure activity relationship analysis of each unique molecule helps to synchronize the compounds with their biological activities as a physical and chemical property [38]. A QSAR modelling involving multiple linear regressions (MLR) analysis was applied to screen potential lead of quinoline and benzofuran analogues against HCT-116 cells. A total number of 28 molecules were subjected to generate a QSAR

model with their physicochemical and topological descriptors such as HBA 1, HBA 2, KAPPA1, KAPPA2, KAPPA3, MW, TPSA, LOGP, MR, LogS, Wiener index and Balaban index. The irrelevant descriptors were removed as outliers. Only four descriptors, including HBA 1, KAPPA1, KAPPA2 and TPSA were involved in generating QSAR model equation. Based on the QSAR analysis from the BuildQSAR tool, HBA1 and KAPPA2 have shown statistical significance that is responsible for the cytotoxicity against HCT-116 cells. The regression coefficient value (r^2 = 0.901) obtained from QSAR analysis, indicated the existence of significant correlation between the inhibitory activity and the chemical descriptors of these derivatives. The descriptors indicate hydrogen bond interactions of the carbonyl groups at C-1 (HBA1), topological Indices and other related descriptors (KAPPA2) [39]. Thus, the results of our study provide a valuable tool in designing new and more potent cytotoxic analogs.

Clustering strategies and similarity measures of compounds are the important aspects of chemoinformatics study. The utility of clustering findings, and the advantages, allow chemists to identify groups of potentially active compounds keeping in view of their bioavailability [40]. The toxicity risk evaluation aims to identify substructures that are indicative of a toxicity risk within the chemical structure [41]. Chemoinformatics based cluster analysis was performed using pharmacophore descriptors of quinoline and benzofuran derivatives. All quinoline ligands were found to have clogP values of below 4, which indicate that they are potent drug candidates within the recommended range, whereas ligands Q2 and Q7 were found to have an irritation effect. Similarly, the cluster analysis of benzofuran ligands indicated that the molecules, B9, B10, B11 and B12 have irritation effect, whereas ligands B11, B10, B9, B12, and B18 were found to have clogP values of more than 5 which violate the rule of five for drug compatibility. Thus, the chemoinformatics study indicated that all the tested quinolines can act as better drug candidates as compared to benzofurans. Among the quinolines, Q9 showed the most desirable SAR values.

The mTOR pathway pedals replication, growth, translation, and along with resilience associated with the tumor. Kumar *et al.* have shown that quinoline derivative is a potent mTOR inhibitor in a cell-based and cell-free mTOR assay [42]. Mechanistically, it was found to be a strong mTOR inhibitor by inducing apoptosis via mitochondrial dependent pathway [43]. In addition, Kundu *et al.*, have shown the validation of a new class of quinoline-based topoisomerase 1 (Top1) inhibitor which possesses the highest human Top1 inhibition activity [44]. Topoisomerase I (PDB ID: 1T8I) is complex with the standard pre-bonded top I poison camptothecin as a co-crystal in a planar geometry with the important residues Arg-364, Asp-533 and Thr-718 in active site of 1T8I. [45]. In our *in-silico* molecular docking studies of quinolines and benzofurans with target receptor mTOR [31] revealed that Q4, Q9 and Q10 possess significant binding interaction with more number of hydrogen bond formation as compared to all the benzofurans. Thus, the quinolines are the class of compounds that have shown promising ability as anticancer agents as revealed by both *in-silico* prediction as well as *in vitro* screening. Based on this, we further carried out docking analysis to determine the binding affinities and interactions of quinoline ligands with the cancer target receptors topoisomerase I [32] and topoisomerase II [33].

Human topoisomerase I (PDB 1T8I) is the molecular target of a diverse set of anticancer compounds having the residues ARG-364, ASP-533 and THR-718, that are implicated in binding to small molecule inhibitors [46]. We thus evaluated the molecular interaction and binding conformations of quinoline ligands (Q1-Q10) which formed the hydrogen bonds and the data clearly indicated that, except Q6, all the quinolines exhibited significant interaction with the favorable residues of topo I receptor. Similarly, the docking results for all the quinoline molecules with topo II DNA complex protein (PDB 1ZXM) revealed that the ligands Q7, Q8, Q9 and Q10 formed hydrogen bonds with the target receptor amino acids. Overall, the data obtained in this study indicated that most of the quinoline derivatives showed better anticancer activity as compared to benzofurans and possessed better docking score by forming conserved hydrogen bonding with important amino acid residues and attaining requisite molecular geometry. All these data revealed that Q9 is the potential hit molecule having most favorable interaction with all the three receptors implicated in binding to anticancer agents.

5. Conclusion

In conclusion, we have identified a novel quinoline ligand Q9, (*N*'-[(6-bromo-2-chloroquinolin-3-yl)methylidene]-2-(4-methylpiperazin-1-yl)acetohydrazide) as a potent and selective inhibitor of mammalian target of rapamycin, topoisomerase I and topoisomerase II. Specifically, our studies revealed that the compound Q9 is highly potent against the proliferation of HCT-116 and MDA-MB-468 carcinomas, and has shown the IC$_{50}$values of 99.6 and 28.94 μM, respectively. The predicted results obtained from QSAR model equation validated the observed and calculated values of activity associated with this class of molecules. The statistically validated QSAR model explains the basis of anticancer activities of compounds. The molecular docking analysis of quinoline derivatives showed high correlation in comparison to the results of the cytotoxic assay. However, further detailed studies are needed with other cancer cell lines to understand its wide applicability. Overall, this study indicated that quinolines are more potent as anticancer agents compared to benzofurans. Further, compound Q9 has emerged as a lead molecule which could be the base for further development and identification of more potent novel and active anticancer agents for clinical use.

Disclosure statement 🔵

Conflict of interests: All authors declare that there are no conflicts of interest associated with the publication of this manuscript.
Author contributions: Rajeshwara Achur, SubbaRao Venkata Madhunapantula and Praveen Kumar conceptualized the study, performed the review of literature and wrote the manuscript. Praveen Kumar carried out bioinformatics analysis and performed the experiments with assistance from Chinnappa Apattira Uthaiah. The synthesis of compounds was carried out by Nayak Devappa Satyanarayan and Santhosha Sangapurada Mahantheshappa. The manuscript contents were designed and compiled in consultation and inputs from Hulikal Shivashankara Santhosh Kumar.
Ethical approval: All ethical guidelines have been adhered.
Sample availability: Samples of the compounds are available from the author.

ORCID 🔵

Praveen Kumar
🔵 http://orcid.org/0000-0002-8034-6348
Chinnappa Apattira Uthaiah
🔵 http://orcid.org/0000-0001-8606-8660

Santhosha Sangapurada Mahantheshappa
ⓘ http://orcid.org/0000-0001-8734-2991
Nayak Devappa Satyanarayan
ⓘ http://orcid.org/0000-0003-4511-3749
SubbaRao Venkata Madhunapantula
ⓘ http://orcid.org/0000-0001-9167-9271
Hulikal Shivashankara Santhosh Kumar
ⓘ http://orcid.org/0000-0003-0371-3535
Rajeshwara Achur
ⓘ http://orcid.org/0000-0001-9867-8917

References

[1]. Bray, F.; Ferlay, J.; Soerjomataram. I.; Siegel, R. L.; Torre, L. A.; Jemal, A. *CA-Cancer J. Clinic.* **2018**, *68(6)*, 394-424.

[2]. Mukherjee, A. K.; Basu, S.; Sarkar, N.; Ghosh, A. C. *Curr. Med. Chem.* **2001**, *8(12)*, 1467-1486.

[3]. Janku, K.; McConkey, D. J.; Hong, D. S.; Kurzrock, R. *Nat. Rev. Clin. Oncol.* **2011**, *8(9)*, 528-539.

[4]. Green, J. A.; Kirwan, J. J.; Tierney. J.; Vale, C. L.; Symonds, P. R.; Fresco, L. L.; Williams, C.; Collingwood, M. *Cochrane Database Syst. Rev.* **2005***, (3)*, CD002225.

[5]. DeVita, V. T.; Chu, E. *Cancer Res.* **2008**, *68(21)*, 8643-8653.

[6]. Chu, X. M.; Wang, C.; Liu, W.; Liang, L. L.; Gong, K. K.; Zhao, C. Y.; Sun, K. L. *Eur. J. Med. Chem.* **2019**, *161*, 101-117.

[7]. Ushio-Fukai, M.; Alexander, R. W. *Mol. Cell Biochem.* **2004**, *264(1-2)*, 85-97.

[8]. Santoshkumar, S.; Satyanarayan, N. D.; Anantacharya, R.; Sameer, P. *Int. J. Pharm. Pharm. Sci.* **2017**, *9*, 260-267.

[9]. Slobbe, P.; Ruijter, E.; Orru, R. V. *Med. Chem. Comm.* **2012**, *3(10)*, 1189-1218.

[10]. Bates, J. G.; Clarke, A.; Kenney, T. F.; Kusam, S.; Tannheimer, S.; Gilead Sciences Inc, assignee. Combination of a bcl-2 inhibitor and a bromodomain inhibitor for treating cancer. United States patent application US 15/790, 434. May 17, 2018.

[11]. Santhosha, S. M.; Synthesis and pharmacological evaluation of novel quinoline derivatives, Ph.D thesis, Kuvempu University, 2017.

[12]. Anantacharya, R.; Manjulatha. K.; Satyanarayan, N. D.; Santoshkumar, S.; Kaviraj, M. Y. *Cogent. Chem.* **2016**, *2(1)*, 1158382.

[13]. Huey, R.; Morris, G. M.; Using AutoDock 4 with AutoDocktools, a tutorial. The Scripps Research Institute, 54-6, 2008, USA.

[14]. Vichai, V.; Kirtikara, K. *Nat. Protoc.* **2006**, *1(3)*, 1112-1116.

[15]. Orellana, E. A.; Kasinski, A. L. *Bio-protocol* **2016**, *6(21)*, e1984.

[16]. De, Oliveira, D. B.; Gaudio, A. C. *Quant. Struct. Act. Relat.* **2000**,*19(6)*, 599-601.

[17]. Dong, J.; Cao, D. S.; Miao, H. Y.; Liu, S.; Deng, B. C.; Yun, Y. H.; Wang, N. N.; Lu, A. P.; Zeng, W. B.; Chen, A. F. *J. Cheminformatics.* **2015**, *7(1)*, 60.

[18]. Smith, R. Y.; Smellie, A.; Mehta, N.; Inventors; PerkinElmer Informatics Inc, assignee. Systems and methods for translating three dimensional graphic molecular models to computer aided design format. *United States patent* US 9,751,294; Sep 5, 2017.

[19]. Gfeller, D.; Grosdidier, A.; Wirth, M.; Daina, A.; Michielin, O.; Zoete, V. *Nucleic Acids Res.* **2014**, *42(W1)*, W32-W38.

[20]. Cheminformatics, M. Calculation of molecular properties and bioactivity score, Retrieved on January 26, 2019, from http://www.molinspiration.com

[21]. Van, Aalten, D. M.; Bywater, R.; Findlay, J. B.; Hendlich, M.; Hooft, R. W.; Vriend, G. *J. Comput. Aided Mol. Des.* **1996**, *10(3)*, 255-262.

[22]. Bernstein, F. C.; Koetzle, T. F.; Williams, G. J.; Meyer, Jr, E. F.; Brice, M. D.; Rodgers, J. R.; Kennard, O.; Shimanouchi, T.; Tasumi, M. *Eur. J. Biochem.* **1977**, *80(2)*, 319-324.

[23]. Goddard, T. D.; Huang, C. C.; Ferrin, T. E. *J. Struct. Biol.* **2007**, *157(1)*, 281-287.

[24]. O'Boyle, N. M.; Banck, M.; James, C. A.; Morley, C.; Vandermeersch, T.; Hutchison, G. R. *J. Cheminformatics.* **2011**, *3(1)*, 33.

[25]. Dallakyan, S.; Olson, A. J. *Methods Mol. Biol.* **2015**, *1263*, 243-250.

[26]. Biovia, D. S. Discovery studio visualizer, San Diego, CA, USA, 2017.

[27]. Willett, P. *Comput. Mol. Sci.* **2011**, *1(1)*, 46-56.

[28]. Hammer, O.; Harper, D. A. T.; Ryan, P. D. *Palaeontol Electron.* **2001**, *4(1)*, 1-9.

[29]. Alam, S.; Khan, F. *Drug Des. Dev. Ther.* **2014**, *8*, 183-195.

[30]. Rahmani, N.; Abbasi-Radmoghaddam, Z.; Riahi, S.; Mohammadi-Khanaposhtanai M. *Struct. Chem.* **2020**, *25*, 1-7.

[31]. Oluiua, J.; Nikolica, K.; Vucicevica, J.; Gagicb, Z.; Filipica, S.; Agbabaa, D.; QSAR modeling and structure based virtual screening of new PI3K/mTOR inhibitors as potential anticancer agents. InCMBEBIH 2017, Proceedings of the International Conference on Medical and Biological Engineering, Vol. 62, p. 379, Springer, 2017.

[32]. Arthur, D. E.; Uzairu, A. *J. Chin. Chem. Soc. Taip.* **2018**, *65(10)*, 1160-1178.

[33]. Chauhan, M.; Joshi, G.; Kler, H.; Kashyap, A.; Amrutkar, S. M.; Sharma, P.; Bhilare, K. D.; Banerjee, U. C.; Singh, S.; Kumar, R. *RSC Adv.* **2016**, *6,* 77717-77734.

[34]. Frisch, M. J.; Trucks G. W.; Schlegel, H. B.; Scuseria, G. E.; Robb, M. A.; Cheeseman, J. R.; Scalmani, G.; Barone, V.; Mennucci, B.; Petersson, G. A.; Nakatsuji, H.; Caricato, M.; Li, X.; Hratchian, H. P.; Izmaylov, A. F.; Bloino, J.; Zheng, G.; Sonnenberg, J. L.; Hada, M.; Ehara, M.; Toyota, K.; Fukuda, R.; Hasegawa, J.; Ishida, M.; Nakajima, T.; Honda, Y.; Kitao, O.; Nakai, H.; Vreven, T.; Montgomery, J. A.; Peralta, J. E.; Ogliaro, F.; Bearpark, M.; Heyd, J. J.; Brothers, E.; Kudin, K. N.; Staroverov, V. N.; Kobayashi, R.; Normand, J.; Raghavachari, K.; Rendell, A.; Burant, J. C.; Iyengar, S. S.; Tomasi, J.; Cossi, M.; Rega, N.; Millam, J. M.; Klene, M.; Knox, J. E.; Cross, J. B.; Bakken, V.; Adamo, C.; Jaramillo, J.; Gomperts, R.; Stratmann, R. E.; Yazyev, O.; A. J. Austin, A. J.; Cammi, R.; Pomelli, C.; Ochterski, J. W.; Martin, R. L.; Morokuma, K.; Zakrzewski, V. G; Voth, G. A.; Salvador, P.; Dannenberg, J. J.; Dapprich, S.; Daniels, A. D.; Farkas, O.; Foresman, J. B.; Ortiz, J. V.; Cioslowski, J.; Fox, D. J. Gaussian, Inc. , Gaussian 09, Revision A. 02, Wallingford CT, 2009.

[35]. Osterberg, F.; Morris, G. M.; Sanner, M. F.; Olson, A. J.; Goodsell, D. S. *Proteins* **2002**, *46(1)*, 34-40.

[36]. Li, H. T.; Zhu, X. *Curr. Top. Med. Chem.* **2020**, *94(7)*, 1396-1417.

[37]. Jin, L. P.; Xie, Q.; Huang, E. F.; Wang, L.; Zhang, B. Q.; Hu, J. S.; Wan, D. C.; Jin, Z.; Hu, C. *Bioorg. Chem.* **2020**, *95*, 103566.

[38]. Singh, A.; Sing, R. *Open Bioinforma. J.* **2013**, *7*, 63-67.

[39]. Li, S.; He, H.; Parthiban, L. J.; Yin, H.; Serajuddin, A. T. *J. Pharm. Sci.* **2005**, *94(7)*, 1396-1417.

[40]. Bocker, A. *J. Chem. Inf. Model.* **2008**, *48(11)*, 2097-2107.

[41]. Bhattacharya, S.; Zhang, Q.; Carmichael, P. L.; Boekelheide, K.; Andersen, M. E. *PloS one.* **2011**, *6(6)*, e20887.

[42]. Kumar, S.; Kumar, Guru, S.; Venkateswarlu, V.; Malik, F.; A, Vishwakarma, R. D.; Sawant, S.; Bhushan, S. *Anti-cancer Agent Me.* **2015**, *15(10)*, 1297-304.

[43]. Venkateswarlu, V.; Pathania, A. S.; Kumar, K. A.; Mahajan, P.; Nargotra, A.; Vishwakarma, R. A.; Malik, F. A.; Sawant, S. D. *Bioorg. Med. Chem.* **2015**, *23(15)*, 4237-4247.

[44]. Kundu, B.; Das, S. K.; Paul, Chowdhuri, S.; Pal, S.; Sarkar, D.; Ghosh, A.; Mukherjee, A.; Bhattacharya, D.; Das, B. B.; Talukdar, A. *J. Med. Chem.* **2019**, *62(7)*, 3428-3446.

[45]. Pal, S.; Kumar, V.; Kundu, B.; Bhattacharya, D.; Preethy, N.; Reddy, M. P.; Talukdar, A.; *Comput. Struct. Biotec.* **2019**, *17*, 291-310.

[46]. Staker, B. L.; Feese, M. D.; Cushman, M.; Pommier, Y.; Zembower, D.; Stewart, L.; Burgin, A. B. *J. Med. Chem.* **2005**, *48(7)*, 2336-2345.